On the Existence of Circle-Point and Center-Point Circles for Three-Precision-Point-Dyad Synthesis[1]

R. J. LOERCH
Graduate Student

A. G. ERDMAN
Assoc. Professor

University of Minnesota, Minneapolis, Minn.

G. N. SANDOR
Research Professor and Director, Mechanical Engineering Design Laboratory, University of Fla.

A graphical method is developed for expressing solutions to all possible revolute dyad, three finitely separated position synthesis problems, where any two rotational displacements are prescribed. Also, cases are discussed where two positions and one velocity are prescribed. The three-precision-point solutions are shown to be represented by circular loci of fixed and moving dyad pivots that are derived from an analytical treatment based on bilinear transformation of the synthesis equations. The superposition of two three-position dyad problems with two common positions yields points on the four-precision-point Burmester curves satisfying both problems. A new alternative explanation for the classical Burmester curve construction is offered. Regions of the plane are found where dyad moving pivots cannot exist for a given problem. Computer graphics output is used to demonstrate several typical solutions.

Introduction

Consider fixed and moving planes connected to a link via revolute joints (Fig. 1(*a*)). Such a configuration is called a revolute dyad and appears in most planar linkages [1, 2, 5, 9, 12]. The four-bar linkage, for example, is composed of two revolute dyads connecting the same fixed and moving planes (Fig. 1(*b*)). Two three-precision-point cases of the moving plane are of interest in this paper:

(1) Case 1 is characterized by moving-plane displacements to two new coplanar positions. A moving-plane tracer point "*P*" undergoes the displacements $\boldsymbol{\delta}_2$ and $\boldsymbol{\delta}_3$ from an initial position $\mathbf{R}_1$ (Fig. 2), while the link rotates by β_2 and β_3, and the moving plane rotates by α_2 and α_3.

(2) Case 2 is characterized by the initial velocity $\mathbf{R}_1$ and one displacement $\boldsymbol{\delta}_2$ of the moving plane tracer point (Fig. 3). The initial angular velocities of the moving plane and the link are $\dot{\alpha}_1$ and $\dot{\beta}_1$ respectively and the moving plane and link rotations to position 2 are α_2 and β_2 respectively.

In two of the usual dyad synthesis tasks (motion generation and path generation with prescribed timing), either $\boldsymbol{\delta}_2$ and $\boldsymbol{\delta}_3$ or $\mathbf{R}_1$ and $\boldsymbol{\delta}_2$ plus two angular parameters are prescribed. Each displacement or velocity condition gives rise to one complex vector loop equation, which contains two scalar equations: one for the real part and one for the imaginary part. The above motions therefore define two vector equations or four scalar equations. From an algebraic synthesis viewpoint, this sytem can be solved only for four reals such as unprescribed vector components or unprescribed angles of rotation.

As shown in Fig. 4, the initial dyad position will be characterized by the vector $\mathbf{R}$ from the initial tracer point position ($\mathbf{R}_1$ is made zero by selecting the origin at the initial tracer point position) to the dyad's fixed pivot and by the vector $\mathbf{W}$ from the fixed pivot to the moving pivot. Thus there are six unspecified parameters ($\mathbf{W}$, $\mathbf{R}$ and two angles of rotation or one angle and one angular velocity), two of which must be additionally pre-

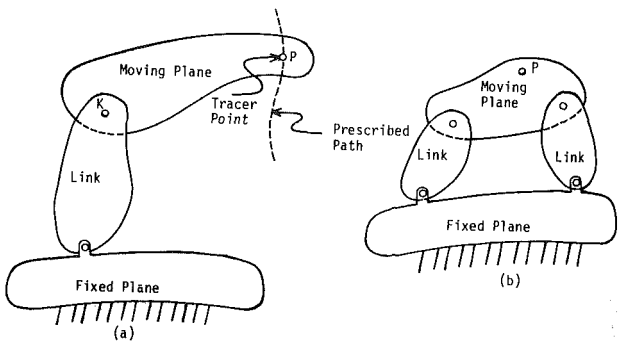

Fig. 1(*a*) Dyad nomenclature

Fig. 1(*b*) Four-Bar linkage made up of two dyads

[1]Based on a Master's thesis by the first author [1].

Contributed by the Mechanisms Committee and presented at the Design Engineering Technical Conference, Minneapolis, Minn., Sept. 24–27, 1978 of the AMERICAN SOCIETY OF MECHANICAL ENGINEERS. Manuscript received at ASME Headquarters June 22, 1978. Paper No. 78-DET-44

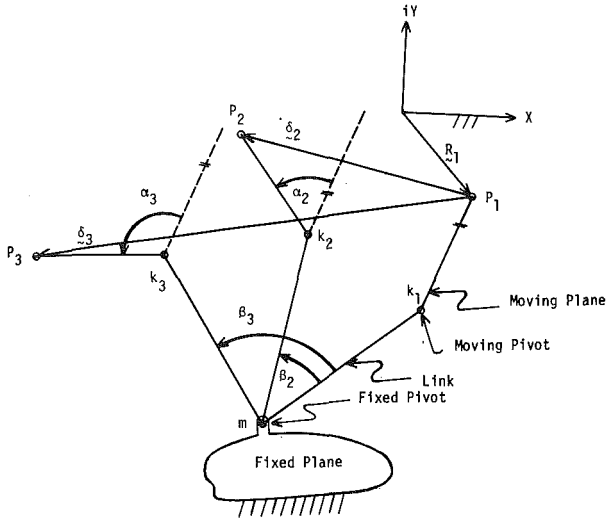

Fig. 2 Case 1: Three finitely separated positions

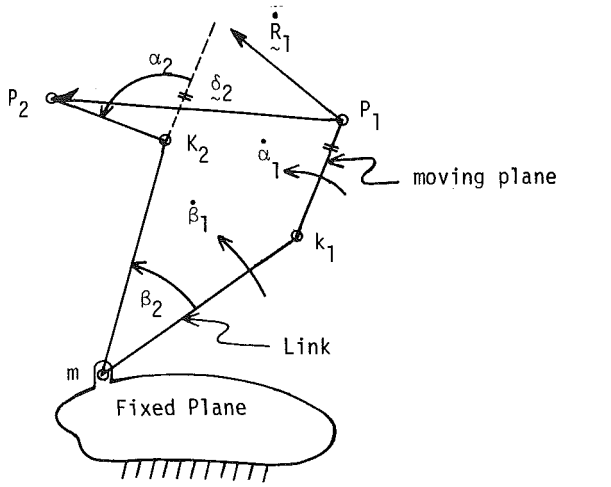

Fig. 3 Case 2: Two infinitesimally close and one finitely separated positions

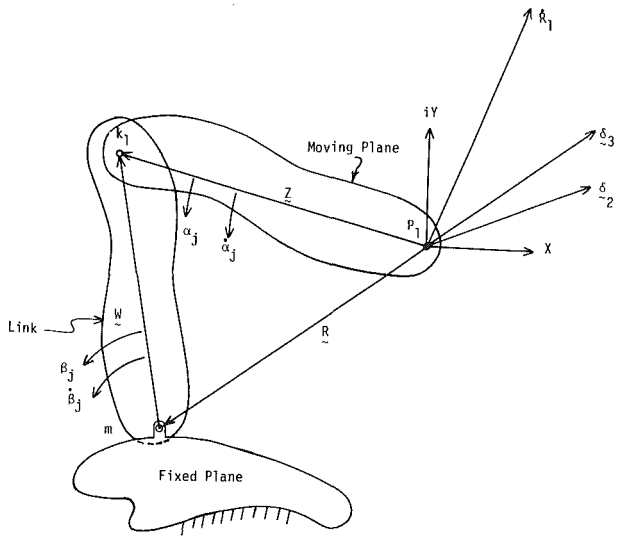

Fig. 4 Vector representation of a dyad

scribed to allow a solution with only four scalar equations. Two different strategies for choosing these two "free choices" have been used thus far. Most commonly, the two remaining angular unknowns (unknown angle or unknown angular velocity) have been picked [9, 12]. This produces a set of linear equations which is easily solvable for **W** and **Z**. Unfortunately, the process of searching for better solutions is difficult when varying the angular parameters in this form. In the second approach, the vector **R** (defining the fixed pivot) is chosen so that each point of the fixed plane can serve as the fixed pivot of a link allowing the prescribed motion [11]. It is impractical, however, to pick all values of **R** and simultaneously show the dyad associated with each choice.

This paper describes a new approach—the angular parameters will be considered as candidates for parameters on which the locations of the fixed and moving pivots of the solution dyads will depend. If an arbitrary value is chosen for one unprescribed angular parameter, while the other parameter is allowed to assume all possible values, the resulting loci of corresponding fixed pivots m and moving pivots k_1 are found to be pairs of circles. For example, if $\mathbf{R}_1$, $\boldsymbol{\delta}_2$, $\boldsymbol{\delta}_3$, α_2, β_2, and β_3 are picked, then the m and k_1 loci trace circles as α_3 ranges between 0 and 2π. Henceforth, moving pivot and fixed pivot circles are referred to as M and K circles, respectively. A complex-number formulation will be used to generate the circles analytically.

Analytical Modelling

Consider a coordinate system at the initial moving plane tracer point position, with vectors defined as in Fig. 4. Using complex numbers, a link rotation θ is accomplished by multiplying the vector defining the link by $e^{i\theta}$, which will be denoted simply by $\boldsymbol{\theta}$. The vector loop equations are:

$$\text{1st position: } \mathbf{R} + \mathbf{W} - \mathbf{Z} = 0 \tag{1}$$

$$\text{2nd Position: } \mathbf{R} + \mathbf{W}\boldsymbol{\beta}_2 - \mathbf{Z}\boldsymbol{\alpha}_2 = \boldsymbol{\delta}_2 \tag{2}$$

$$\text{3rd Position: } \mathbf{R} + \mathbf{W}\boldsymbol{\beta}_3 - \mathbf{Z}\boldsymbol{\alpha}_3 = \boldsymbol{\delta}_3 \tag{3}$$

$$\text{1st Velocity: } \mathbf{W}i\dot{\beta}_1 - \mathbf{Z}i\dot{\alpha}_1 = \dot{\mathbf{R}}_1, \tag{4}$$

$$\text{where} \quad i \equiv \sqrt{-1}$$

Subtracting equation (1) from equations (2) and (3) yields the "standard form" equations [(9), (12)] for three-position synthesis:

$$\mathbf{W}(\boldsymbol{\beta}_2 - 1) - \mathbf{Z}(\boldsymbol{\alpha}_2 - 1) = \boldsymbol{\delta}_2 \tag{2a}$$

$$\mathbf{W}(\boldsymbol{\beta}_3 - 1) - \mathbf{Z}(\boldsymbol{\alpha}_3 - 1) = \boldsymbol{\delta}_3 \tag{3a}$$

As stated above, the usual technique of solving a three-position synthesis task using (2a) and (3a) is to inspect dyads obtained by randomly varying the unprescribed angles in equations (2a) and (3a) (solving for **W** and **Z** via Cramer's rule). It was observed here that, if one unprescribed angle is fixed while the other is systematically varied, the fixed and moving pivots of the resulting dyads each describe a circular locus: the M-circle for the fixed pivots and the K-circle for the moving pivots. The circumscribing circles of the pole triangle and the image pole triangle discussed in [4] are special cases of these circles.

In equation (1), the location of the moving pivot is defined by the vector **Z** with respect to the origin of the coordinate system which, as shown in Fig. 4, conincides with the initial position P_1 of the tracer point of the moving plane. Synthesis problems can be formulated by specifying $\boldsymbol{\delta}_2$ and $\boldsymbol{\delta}_3$, or $\dot{\mathbf{R}}_1$ and $\boldsymbol{\delta}_2$ plus the appropriate angular parameters. Vectors **R** and **Z** may be obtained from either equations (1, 2, 3) or (1, 2, 4) (using Cramer's Rule).

When $\boldsymbol{\delta}_2$ and $\boldsymbol{\delta}_3$ are specified, equations (1, 2, 3) yield

$$R = \frac{\begin{vmatrix} 0 & 1 & -1 \\ \delta_2 & \beta_2 & -\alpha_2 \\ \delta_3 & \beta_3 & -\alpha_3 \end{vmatrix}}{\begin{vmatrix} 1 & 1 & -1 \\ 1 & \beta_2 & -\alpha_2 \\ 1 & \beta_3 & -\alpha_3 \end{vmatrix}} \tag{5}$$

or

$$R = \frac{-\delta_2(\beta_3 - \alpha_3) + \delta_3(\beta_2 - \alpha_2)}{-(\alpha_2 - \alpha_3 + \beta_3 - \beta_2) - \beta_2\alpha_3 + \alpha_2\beta_3} \tag{6}$$

and

$$Z = \frac{\begin{vmatrix} 1 & 1 & 0 \\ 1 & \beta_2 & \delta_2 \\ 1 & \beta_3 & \delta_3 \end{vmatrix}}{\begin{vmatrix} 1 & 1 & -1 \\ 1 & \beta_2 & -\alpha_2 \\ 1 & \beta_3 & -\alpha_3 \end{vmatrix}} \tag{7}$$

or

$$Z = \frac{-\delta_2(\beta_3 - 1) + \delta_3(\beta_2 - 1)}{\beta_2 - \beta_3 + \alpha_3 - \alpha_2 - \beta_2\alpha_3 + \alpha_2\beta_3} \tag{8}$$

When $\dot{R}_1$ and δ_2 are specified, equations (1, 2, 4) yield

$$R = \frac{\dot{R}_1(\beta_2 - \alpha_2) + \delta_2(\dot{\alpha}_1 - \dot{\beta}_1)}{-\alpha_2\dot{\beta}_1 - \dot{\alpha}_1 + \dot{\beta}_1 + \dot{\alpha}_1\beta_2} \tag{9}$$

$$Z = \frac{-\dot{R}_1 i + \beta_2\dot{R}_1 i - \dot{\beta}_1\delta_2}{-\dot{\beta}_1\alpha_2 + \dot{\beta}_1 - \dot{\alpha}_1 + \beta_2\alpha_1} \tag{10}$$

If all parameters on the right sides of these expressions are fixed except one angular parameter θ, which ranges over all possible values, the equations for R and Z can be expressed as functions of θ to form "bilinear mappings" [3]:

$$R(\theta) = \frac{a\theta + b}{c\theta + d} \tag{11}$$

$$Z(\theta) = \frac{e\theta + f}{g\theta + h} \tag{12}$$

where $a \rightarrow h$ are known and $\theta = e^{i\theta}$, and where θ stands for the angle to be varied (β_2, α_2 or β_3) or the angular velocities ($\dot{\beta}_1$ or $\dot{\alpha}_1$).

When θ varies from 0 to 2π, θ describes the unit circle. Equations (11) and (12) are tantamount to the following sequence of transformations:

$$p(\theta) = a\theta, \quad \text{a stretch rotation,} \tag{13}$$

$$q(\theta) = a\theta + b, \quad \text{a change of origin,} \tag{14}$$

$$r(\theta) = c\theta, \quad \text{another stretch rotation,} \tag{15}$$

$$s(\theta) = c\theta + d, \quad \text{another change of origin, and} \tag{16}$$

$$t(\theta) = \frac{q(\theta)}{s(\theta)} \quad \text{a "bilinear mapping"}$$

Since both $q(\theta)$ and $s(\theta)$ are circles, it can be shown that $t(\theta)$ is also a circle (reference [3]). Thus, it is seen that the loci of $R(\theta)$ and $Z(\theta)$ are circles, which in the limit can become straight lines. The complex constants a through h are found by appropriately rearranging equations (6) and (8) or (9) and (10) in the form of equations (11) and (12). The centers of the circular loci M and K can be found directly from the constants a through h [1], or more simply by evaluating R and Z at three θ values, yielding three points. Either way the solutions are within the realm of programmable hand calculators. Computer programs have been written to display the M and K circles on a TEKTRONIX 4013 graphics terminal [10] in order to examine their properties. This led to the manual graphical constructions presented in the next section.

When the circles have been drawn, it remains to coordinate associated fixed and moving pivots on a pair of circles. This is done using the well known pole or instant-center relationships presented in Figs. 5 and 6, respectively. For example, rays emanating from P_{12} defining an angle $1/2\ \alpha_2$ will intersect the M and K circles at fixed and moving pivot pairs m and k_1. An angle meter (adjustable protractor) rotated about the coordinating pole or instant center serves as a convenient tool for revealing such pivot pairs.

Graphical Constructions: Two-Displacement Problems

Here δ_2, δ_3, and two rotations are prescribed. Names have been assigned according to which rotations are chosen:

Prescribed angles	Name	MK circle pairs generated for different values of
α_2 α_3	Motion generation	β_2
β_2 β_3	Path generation (with prescribed timing)	α_2
β_2 α_3	Path generation (with opposite angles prescribed)	β_3

Sample computer plots have been generated for each of the

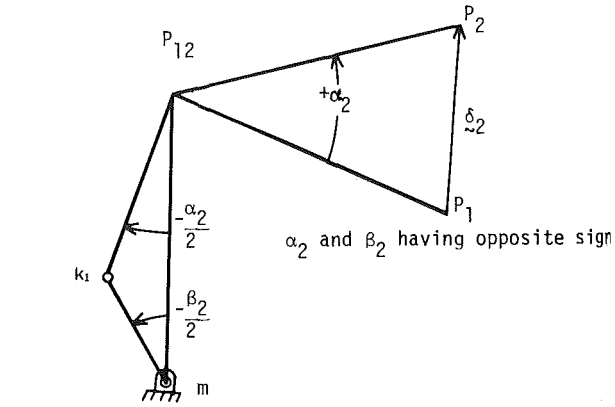

Note: -180 < angles < 180

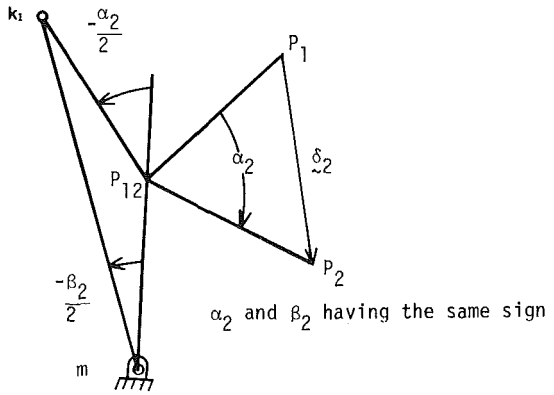

Fig. 5 Pole, circlepoint and centerpoint relationship

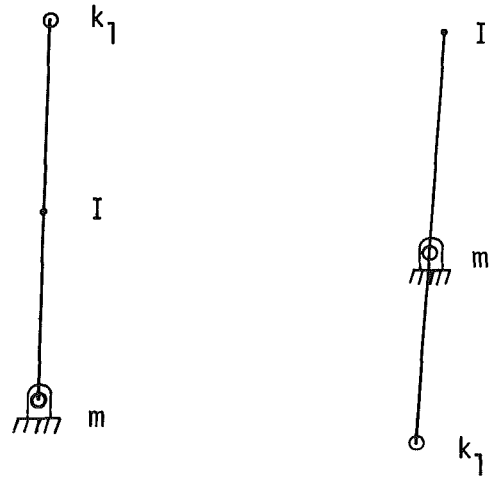

$\dot{\alpha}$ and $\dot{\beta}$ of Same Sign

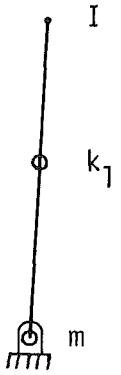

$\dot{\alpha}$ and $\dot{\beta}$ of Opposite Sign

Fig. 6 Instant center, circlepoint and centerpoint relationship

three problem types (Figs. 7, 8, and 9). The M circles (with solid arcs) are labeled with the values of the angle varied to generate them. A short line segment is directed from a sample fixed pivot m on each M circle toward the moving pivot k_1 on the associated K circle (with dashed arcs). If this moving pivot lies off the diagram, the K circle is also labeled with the value of the angle varied to generate it. The poles used in finding conjugate $m - k_1$ pairs are represented by small rings.

In path generation with prescribed timing, the pole P_{12} to be used for finding conjugate pivots on each MK circle pair will be different for each such pair, since neither α_2 nor α_3 is the same for different pairs. A shorter line segment is then directed from the sample fixed pivot of each M circle toward the associated pole P_{12} (see Fig. 8).

Motion Generation. Fig. 7 illustrates a motion generation example. X_1, X_2 and X_3 mark the prescribed positions of the tracer point P, with $\delta_2 = 1 + i$, $\delta_3 = 2 + 0.5i$, $\alpha_2 = 1$ rad and $\alpha_3 = 2$ rad.[2] The M and K circles are generated for three values of the

[2]Counterclockwise rotations are positive.

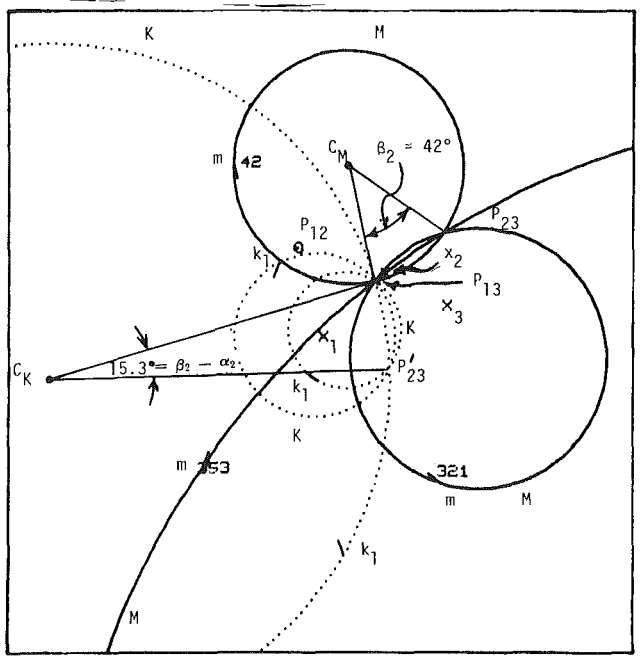

Fig. 7 Circlepoint and centerpoint circles for motion generation

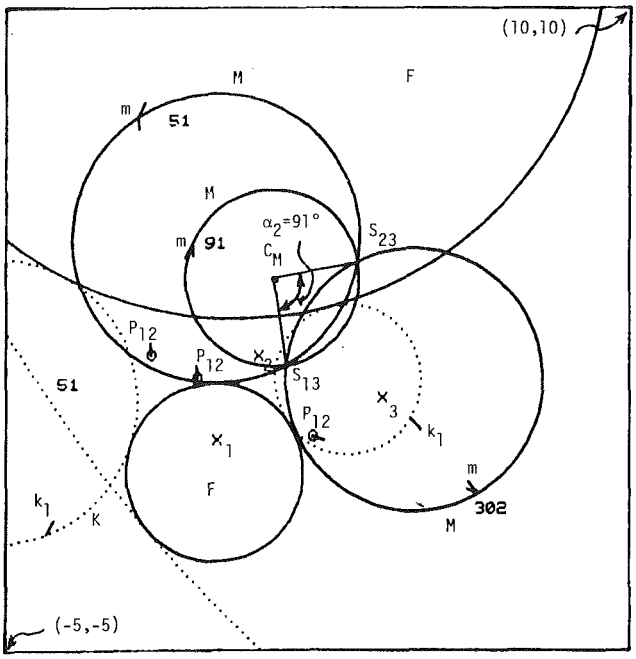

Fig. 8 Circlepoint and centerpoint circles for path generation with prescribed timing

varied angle β_2(42°, 321° and 353°), with β_3 ranging from 0 to 2π. These three circle-point circles and center-point circles are sufficient to display the properties of the diagram. It is interesting to note that the M and K circles intersect at points which can be shown to be the poles P_{13} and P_{23} for the M circles and P_{13}, P'_{23} for the K circles, where P'_{23} is the image pole of P_{23}. Similarly notable are the angles subtended by the intersections at the circle centers (see Fig. 7). The steps needed to construct a set of circular M and K loci for a motion generation problem are therefore:

(1) Find the circle-intersection poles: P_{13} and P_{23} for the M circles; P_{13} and P'_{23} for the K circles.

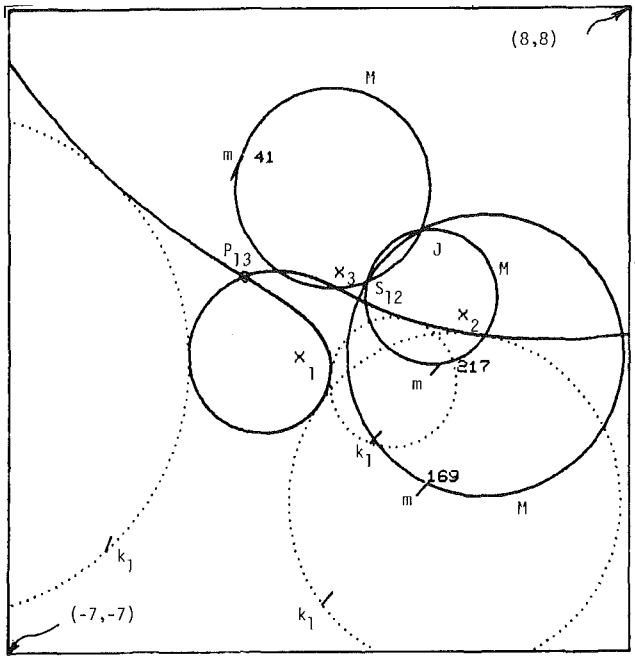

Fig. 9 Circlepoint and centerpoint circles for path generation with opposite angles prescribed

(2) Bisect the lines between the intersection pole pairs to find the lines of centers for the M and K circles.

(3) For each value of the varied angle β_2, lay off the circle centers so that

$$\measuredangle P_{13}C_MP_{23} = \beta_2 \quad \text{and} \quad \measuredangle P_{13}C_KP'_{23} = \alpha_2 - \beta_2$$

(4) Draw the circle pairs with centers C_M and C_K through the intersection poles. It can be shown that the complex number expressions for the poles are:

$$\mathbf{P}_{12} = \frac{\boldsymbol{\delta}_2}{1 - \boldsymbol{\alpha}_2}, \tag{18}$$

$$\mathbf{P}_{13} = \frac{\boldsymbol{\delta}_3}{1 - \boldsymbol{\alpha}_3} \quad \text{and} \tag{19}$$

$$\mathbf{P}_{23} = \frac{\boldsymbol{\delta}_3\boldsymbol{\alpha}_2 - \boldsymbol{\delta}_2\boldsymbol{\alpha}_3}{\boldsymbol{\alpha}_2 - \boldsymbol{\alpha}_3}, \tag{20}$$

where $\mathbf{P_{ij}}$ is the vector from the origin of $\mathbf{R_i}$ to the pole P_{ij}

Path Generation With Prescribed Timing. An example of path generation with prescribed timing is shown in Fig. 8, with $\boldsymbol{\delta}_2 = 1 + 2i$, $\boldsymbol{\delta}_3 = 4 + i$, $\beta_2 = 1$ rad and $\beta_3 = 2$ rad. The M and K circles are generated for $\alpha_2 = 51°$, 91° and 302°, with α_3 ranging from 0 to 360°. The M circles all have common intersections at the pseudo-poles[3] S_{13} and S_{23}, and exhibit properties that allow M circle construction with the steps used in motion generation, except that the varied angle is α_2 rather than β_2.

The K circles have no intersections, but a useful property exists that permits easy K circle construction: the M and K circle centers are coordinated about the poles as are the m and k_1 pivots (see Fig. 5). Referring to Fig. 10, C_K and k_1 (the moving pivot corresponding to either fixed pivot on the M circle diameter through P_{12}) are found accordingly, allowing the K circle to be drawn about C_K with radius $|C_Kk_1|$.

The M and K circles of path generation with prescribed timing can be found as follows:

(1) Construct the M circles in a manner similar to that used in motion generation, but vary α_2 to obtain different circles.

[3]The pseudo-poles are defined as poles with rotations β rather than α.

(2) For each M circle:

(a) Construct the pole P_{12}.

(b) Draw the diameter of the M circle through P_{12} and extend it.

(c) From this line, lay off the angle $\alpha_2/2$ with P_{12} as the apex, and the angle $\beta_2/2$ with C_M as the apex. The intersection of these two lines is C_K. Choose the intersections of the C_MP_{12} line with the M circle to be the fixed pivot m. With this point as the apex lay off the angle $\beta_2/2$ from the $P_{12}C_Mm$ line. The intersection of this line with the $\alpha_2/2$ line is k_1, and the K circle can now be formed. (See Fig. 10.)

Path Generation With Opposite Angles Prescribed. With β_2 and α_3 prescribed, circle sets can be generated for discrete values of β_3 by letting α_2 range from 0 to 360°. Fig. 9 shows an example [$\boldsymbol{\delta}_2 = (4 + i)$, $\boldsymbol{\delta}_3 = (1 + 2i)$, $\beta_2 = 2$ rad, $\alpha_3 = 1$ rad with M and K circles for $\beta_3 = 41°$, 169° and 217°.] The resulting M circles appear similar to those of motion and path generation; however, one of the M circle intersection points must be located indirectly, because the angle subtended from the M circle centers by the intersection points is not the varied angle β_3 [1]. The graphical procedure is as follows:

(1) On the perpendicular bisector of $\mathbf{R}_1 - \mathbf{R}_3$ locate the pseudo-pole Q_{13} with rotation β_2. Similarly locate S_{12} (see Fig. 11).

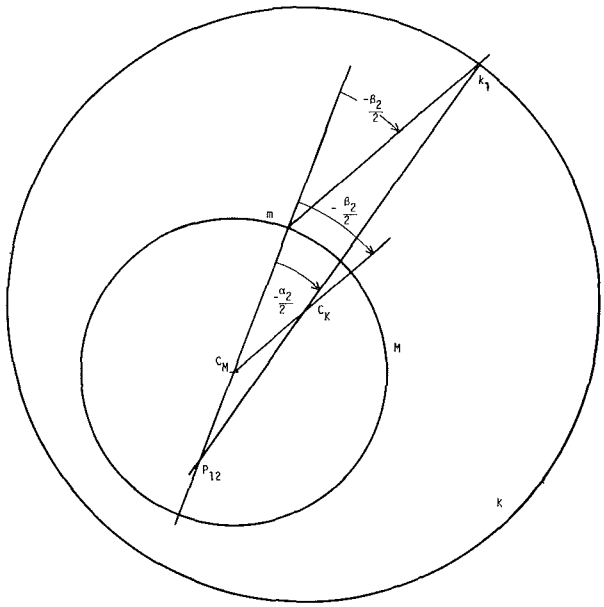

Fig. 10 K circle construction for path generation with prescribed timing

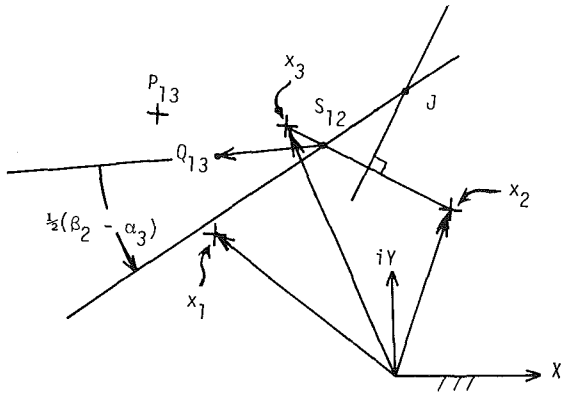

Fig. 11 M circle intersection construction for path generation with opposite angles prescribed

(2) Draw the $S_{12}Q_{13}$ line and from it lay off the angle $(1/2)(\beta_2 - \alpha_3)$. The intersection of the resulting line with the perpendicular bisector of $\mathbf{R}_2 - \mathbf{R}_3$ is the point J. This point together with pseudo-pole S_{12} form the pair of common intersections of all M circles.

Given S_{12} and J, M circles can be drawn, but the $\beta_3 - M$ circle correspondence is unavailable. Fortunately, however, the M circle intersections with the $(\mathbf{R}_3 - \mathbf{R}_2)$ bisector are the pseudo-poles S_{25}, yielding β_{23}, and $\beta_3 = \beta_2 + \beta_{23}$. C_M, α_3, β_3, and P_{13} are now known; each K circle center and radius can now be found using the pole relationship of Fig. 5 as in path generation.

Dyad Moving Pivot Existence - Three Precision Points

When computer plots of the M and K circles were made, it was found that moving pivots cannot exist within certain regions of the plane in path generation with prescribed timing or with opposite angles prescribed.

For path generation with prescribed timing, two circles exist within which no moving pivots will be found. One of the circles surrounds the first moving point position and it is possible to analytically define a distance bound from this point, within which no moving pivots can exist. All K circles are tangent to both existence circles and are arranged so that two k_1 pivot solutions occur for each point outside the circles. In addition to Fig. 8, Fig. 12 shows the nonexistence circles (labeled as "F" for forbidden regions), for the example:

$$\boldsymbol{\delta}_2 = 2 + 2i; \qquad \beta_2 = 0.5 \text{ radians}$$

$$\boldsymbol{\delta}_3 = 4 + i; \qquad \beta_3 = 1 \text{ radian}$$

The circles shown are the K circles which are tangent to the two non-existence circles, the smaller surrounding the initial precision point, X_1 in Fig. 12.

For path generation with opposite angles prescribed, an algebraic curve exists, to one side of which no moving pivots are found. Each K circle is tangent to this curve at least once, and again the K circles are arranged to give two moving pivot solutions for each point within the permissible regions. In addition to Fig. 9, Fig 13 shows an example where

$$\boldsymbol{\delta}_2 = 2 + 1i; \qquad \beta_2 = 1 \text{ radian}$$

$$\boldsymbol{\delta}_3 = -2 + 4i; \qquad \alpha_3 = 1 \text{ radian}$$

Again, the areas labeled "F" are the forbidden or nonexistence regions. Expressions for both these moving pivot existence region boundaries have been derived in [1].

Four Prescribed Positions: Superposition of Two Three-Precision-Point Cases

Consider the four-position motion synthesis problem with $\boldsymbol{\delta}_2$, $\boldsymbol{\delta}_3$, $\boldsymbol{\delta}_4$, α_2, α_3 and α_4 prescribed. This can be considered as a superposition of two three-position, motion generation subproblems, with ($\boldsymbol{\delta}_2$, $\boldsymbol{\delta}_3$, α_2, α_3) prescribed in one and ($\boldsymbol{\delta}_2$, $\boldsymbol{\delta}_4$, α_2, α_4) prescribed in the other. For a selected value of the varied angle β_2, an M and K circle can be drawn for each subproblem; M circle intersections and K circle intersections define points that satisfy both subproblems simultaneously.

For example, suppose the following sets of precision positions were desired:

Set 1

$$\boldsymbol{\delta}_2 = 2 + 2i \qquad \alpha_2 = 60°$$

$$\boldsymbol{\delta}_3 = 5 + 2i \qquad \alpha_3 = 120°$$

Set 2

$$\boldsymbol{\delta}_2 = 2 + 2i \qquad \alpha_3 = 60°$$

$$\boldsymbol{\delta}_4 = 4 + 3i \qquad \alpha_4 = 180°$$

The intersections of the corresponding M circles and K circles from both three-point problem define the four-precision-point-"Burmester curves": the "circle-point" and "center-point" curves.

One begins by finding the intersection poles P_{12}, P_{13}, P_{23}, P_{24}, P'_{23}, and P'_{24}. There will be two sets of M and K circles, labeled

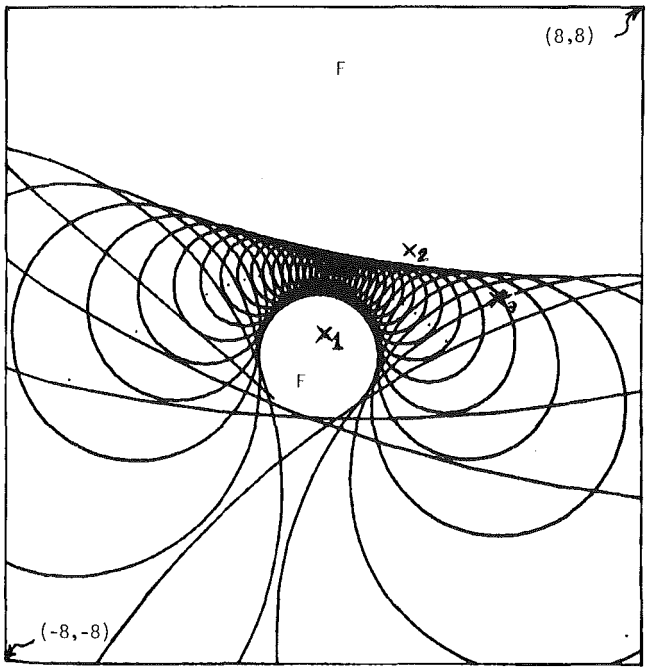

Fig. 12 Example of path generation with prescribed timing showing nonexistence circles labeled as F ("forbidden regions")

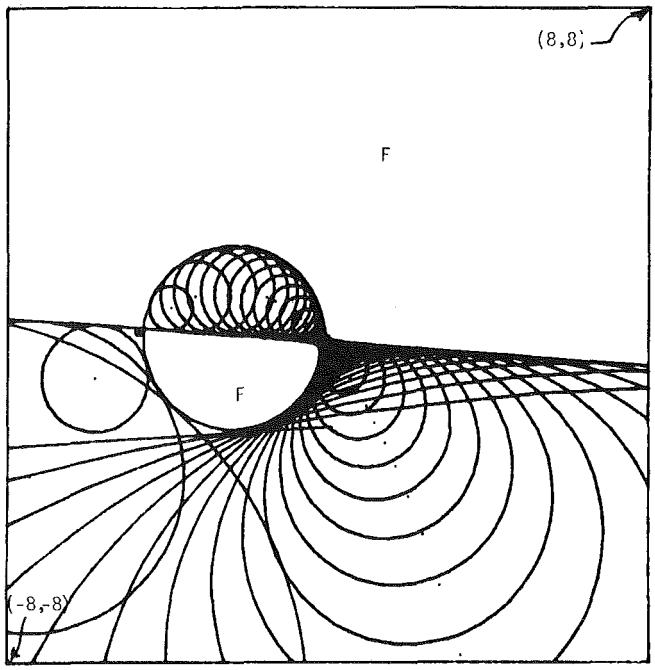

Fig. 13 Example of path generation with opposite angles prescribed showing nonexistence regions labeled as F ("forbidden regions")

with superscripts (M^1 corresponds to set 1). The centers of circles M^1, M^2, K^1, K^2 lie on the bisectors of P_{13} P_{23}, P_{14} P_{24}, P_{13} P'_{23}, and P_{14} P'_{24} respectively, as shown in Fig. 14. Note that the following length equalities prevail:

$$|P_{13}P_{23}| = |P_{13}P'_{23}| \tag{21}$$

and

$$|P_{14}P_{24}| = |P_{14}P'_{24}| \tag{22}$$

Up to eight M and K curve points can be found for each value of ϵ, the positive angle subtended by the respective pole distances at the corresponding circle centers. For $\epsilon = 40°$, one draws (Fig. 14) four arcs with radius $1/2|P_{14}P_{24}|\csc(\epsilon/2)$ from rays[4] K^{1+}, K^{1-}, M^{1+} and M^{1-}, followed by their respective intersections with arcs of radius 3.9 from the rays K^{2+}, K^{2-}, M^{2-}, M^{2+}, and M^{2-}. Since the M^{1-} arcs do not intersect the M^{2-} arcs for the particular example, they are omitted. The varied angles corresponding to each intersection pair are (two arcs may intersect at two points):

$$M^+: \quad \beta_2 = +\epsilon = +40°$$

$$K^+: \quad \beta_2 = \alpha_2 - \epsilon = 60° - 40° = 20°$$

$$K^-: \quad \beta_2 = \alpha_2 - (-\epsilon) = 60° + 40° = 100°$$

The K^+ and the K^- intersections apply for β_2 less than α_2 or β_2 greater than α_2, respectively. Note, for example, that if one desired the moving pivots for $\beta_2 = 40°$, they would be the K^+ intersections for $\epsilon = \alpha_2 - \beta_2 = 20° > 0$.

This procedure, derived here from the three-position M and K circles, is the same as the Burmester curve construction based on the opposite pole quadrilateral [2, 4]. For example, the M curve points are found as the intersections of circles with opposite pole quadrilateral sides as chords, which is identical to the construction used here. In popular kinematic texts [2, 4, 5, 6, 7], however, these circles are not presented as three-point solution loci, but as loci of points that subtend equal or supplementary angles at the side of the opposite-pole quadrilateral representing the chord of the circle. The intersections of circles through opposite-pole pairs whose peripheral points subtend equal or supplemantary angles at their respective chords are constructed; these points satisfy the theorem of Burmester, which states that the points on the M curve subtend equal or supplemental angles at opposite sides of the opposite-pole quadrilateral.

[4]The plus or minus sign in the superscripts of the rays indicates one direction or the other towards infinity.

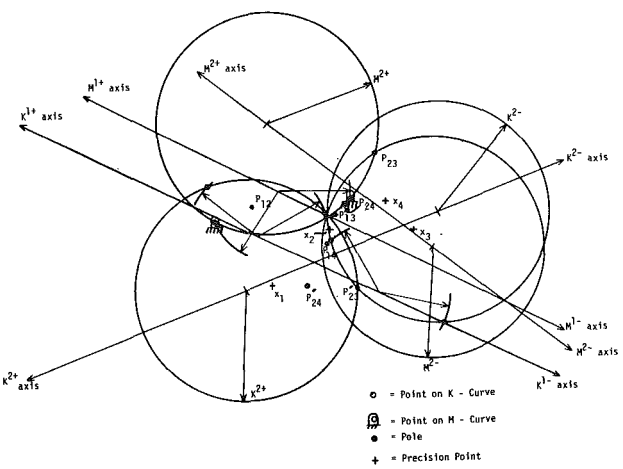

Fig. 14 Construction for four finitely separated prescribed positions for motion generation

A more direct statement based on the present work might be: Each circle-pair intersection represents the superposition of two three-point synthesis problems with prescribed quantities (δ_2, δ_3, α_2, α_3) and (δ_2 δ_4, α_2, α_4) respectively, together comprising the four-point problem.

Although the opposite-pole quadrilateral construction technique is well known, this is the first time (to the authors' knowledge) that a kinematic derivation of the graphical Burmester curve generation technique has been introduced.

Dyad Moving-Pivot Existence - Five Precision Points

For path synthesis problems with more than three precision points, two moving-pivot nonexistence circles will result for each distinct combination of three precision points. Thus a four-point problem will have six such circles, while a five-point problem will have twelve. Moving-pivot solutions will not exist inside these circles. Consider for example a five-point Burmester path synthesis [8, 14] with four displacements and corresponding link rotations given:

$$\delta_2 = 2 + 2i, \quad \beta_2 = 60° \qquad \delta_3 = 5 + 2i, \qquad \beta_3 = 120°$$

$$\delta_4 = 4 + 4i, \quad \beta_4 = 180° \qquad \delta_5 = -2 + 2i, \quad \beta_5 = 240°$$

Each pair of prescribed displacements defines two nonexistence circles; the twelve circles and the Burmester dyad solutions are shown in Fig. 15. The dyads shown are the only solutions available. Note that the moving pivots of these dyads are external to all nonexistence circles.

Graphical Construction: Displacement and Velocity Problems

Here R_1, δ_2, β_2 or α_2, and $\dot{\beta}_1$ or $\dot{\alpha}_1$ are prescribed. The problem types are (see Fig. 3):

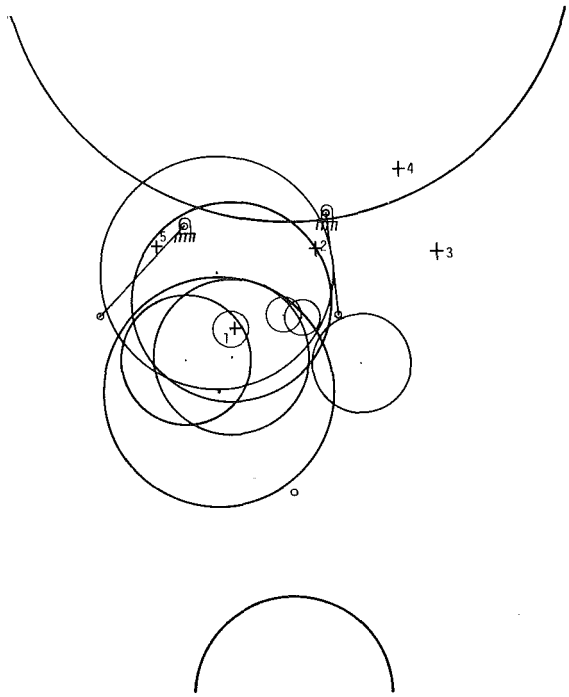

Fig. 15 Nonexistence circles for path generation with prescribed timing for five finitely separated positions

Angle and angular velocity prescribed		Name
α_2	$\dot{\alpha}_1$	Motion generation
β_2	$\dot{\beta}_1$	Path generation with prescribed timing
α_2	$\dot{\beta}_1$	Path generation Type II
β_2	$\dot{\alpha}_1$	Path generation Type III

Motion Generation. In Fig. 16, M and K circles are generated for several values of β_2. I_1 is the instant center on the perpendicular to $\dot{\mathbf{R}}_1$ drawn from X_1; P_{12} is the rotation pole for the displacement δ_2, α_2. The C_K and C_M center loci both coincide with the perpendicular bisector of $P_{12}I_1$. The centers are situated like 'poles of poles' that rotate I_1 to P_{12} about C_K and C_M, the angles of rotation being β_2 and $\beta_2 - \alpha_2$ respectively. To correlate m and k pivots, lines are drawn across the circle pairs though I_1; the circle-line intersections are pivots belonging to the same link. Two sets of these are shown in the figure.

Path Generation With Prescribed Timing. Fig. 17 shows pairs of M and K circles generated for several values of $\dot{\alpha}_1$. All M circles pass through the pseudo-pole S_{12}; each is tangent to the same line through it. The M circle radii are proportional to the ratios $\dot{\beta}_1/\dot{\alpha}_1$. The instant center I_1, C_m, C_k all lie on one line. When $\dot{\alpha}_1 = \dot{\beta}_1$, the corresponding M circle passes through S_{12} and I_{S1}, with its center at C_m, where I_{S1} is the pseudo-instant center with angular velocity β_1.

The construction procedure for the path generation with prescribed timing and discussion of the other two path generation cases [1] will not be presented here due to lack of space but will be a part of a future publication.

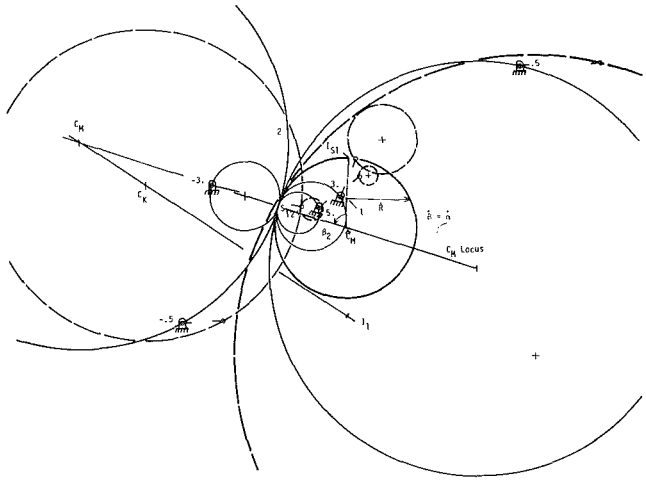

Fig. 17 Example of path generation with prescribed timing for two infinitesimally close and one finitely separated positions

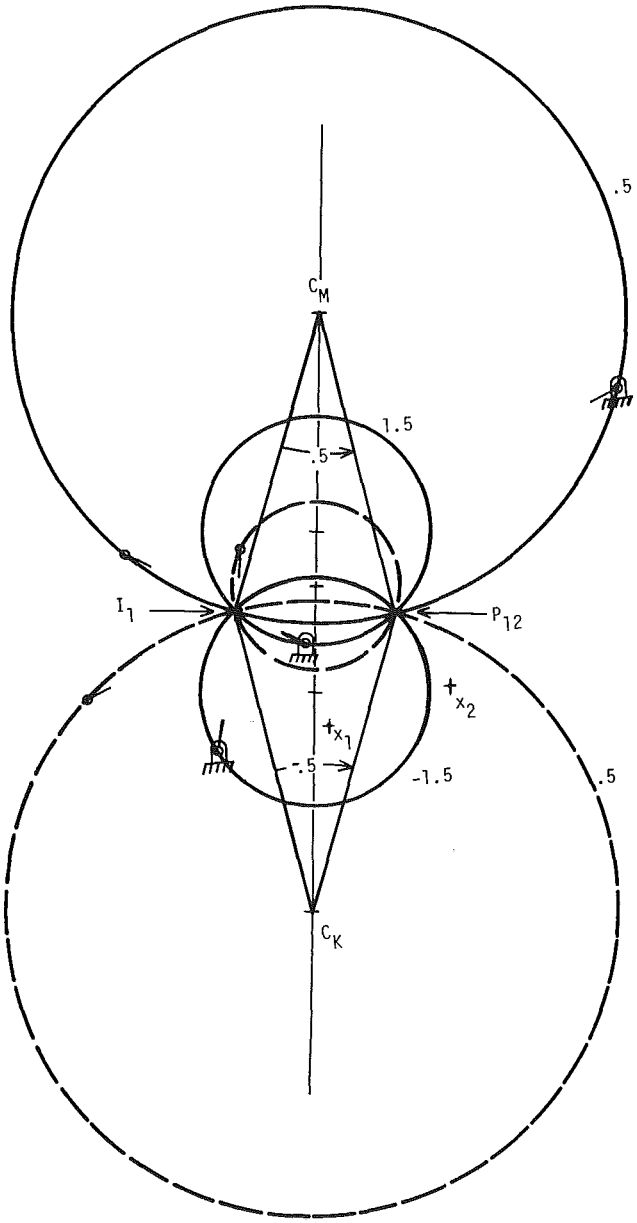

Fig. 16 Example of motion generation for two infinitesimally close and one finitely separated positions

Conclusion

A complex-number dyadic method of planar body-guidance synthesis has been presented. It was discovered that, for three precision conditions, with one unprescribed angle fixed and the other used as a parameter, fixed pivots m and moving pivots k_i of all possible dyads must lie on respective circular loci, named the "M circles" and "K circles." There is one such pair of M and K circles for each assumed value of the first unprescribed angle. When the task is path generation with prescribed timing or with prescribed opposite angles, regions have been found within which no moving pivots can exist. These were named "nonexistence regions"; they are envelopes of the K circles. Graphical methods based on this theory give rise to a new, kinematic derivation of the well known geometric construction of Burmester's center-point and circle-point curves for four prescribed positions, and of the (up to) four discrete Burmester Point Pairs for five prescribed positions. The methods have been programmed for interactive computer graphics.

Acknowledgment

The first two authors wish to acknowledge support of the University Computer Center, University of Minnesota. The third author wishes to acknowledge support under NSF Grant ENG 76-03894 A01, sponsored by the Solid Mechanics Program in the Engineering Division of the National Science Foundation.

References

1 Loerch, R. J., "Extensions of Revolute Dyad Synthesis for Three Finitely Displaced Positions," M.S. thesis, University of Minnesota, July, 1977.

2 Hartenberg, R. S., and Denavit, J., *Kinematic Synthesis of Linkages*, McGraw-Hill Book Company, New York, 1964.

3 Goodstein, R. L., *Complex Functions*, McGraw-Hill Ltd., Maidenhead, England, 1965.

4 Beyer, R., *Kinematic Synthesis of Mechanisms,* translated by Kunzel, Chapman and Hall Ltd., London.
5 Hain, K., *Applied Kinematics,* 2nd edition, McGraw-Hill Book Company, Inc., New York, 1967.
6 Tao, D. C., *Applied Linkage Synthesis,* Addison-Wesley, Reading, Massachusetts, 1964.
7 Hall, A. S., Jr., *Kinematics and Linkage Design,* Prentice-Hall, Inc., Englewood Cliffs, New Jersey, 1961.
8 Freudenstein, F., and Sandor, G. N., "Synthesis of Path Generating Mechanisms by Means of a Programmed Digital Computer," ASME, *Journal of Engineering for Industry,* Vol. 81, No. 2, May, 1959.
9 Erdman, A. G., and Sandor, G. N., *Mechanism Design: Analysis and Synthesis,* to be published by Prentice-Hall, 1979.
10 *Tektronix Plot 10 Terminal Control System User Manual,* Tektronic, Inc., Beaverton, Oregon, 1977.
11 Loerch, R. J., Erdman, A. G., Sandor, G. N., and Midha, A., "Synthesis of Four-bar Linkages with Specified Ground Pivots," *Proceedings of the 4th OSU Applied Mechanisms Conference,* Nov. 2-5, 1975, Chicago, pp. 10–1 to 10–8.
12 Rao, A., Erdman, A. G., Sandor, G. N., et. al., "Synthesis of Multi-Loop Dual-Purpose Planar Mechanisms Utilizing Burmester Theory," *Proceedings, 2nd OSU Applied Mechanism Conference,* Stillwater, Oklahoma, Oct. 7–9, 1971, pp. 7–1 to 7–25.
13 Keller, R. E., "Sketching Rules for the Curves of Burmester Mechanisms Synthesis," Paper No. 64-MECH-5, Trans. *ASME,* Lafayette, In., Oct. 19–21, 1964, six pages.
14 Sandor, G. N., "A General Complex-Number Method for Plane Kinematic Synthesis with Applications," *Doctoral Dissertation,* Columbia University, University Microfilms, Ann Arbor, Michigan, 305 pp., Library of Congress Card No. 59-2596, 1959.
15 Freudenstein, F., and Sandor, G. N., "On the Burmester Points of a Plane," ASME, *Journal of Applied Mech.,* Trans. ASME, Vol. 28, No. 3, Sept. 1961, pp. 473–475.